

Article

UVC Up-Conversion and Vis-NIR Luminescence Examined in SrO-CaO-MgO-SiO₂ Glasses Doped with Pr³⁺

Olha Bezkravna ^{1,2}, Radosław Lisiecki ¹, Bogusław Macalik ¹ and Przemysław Jacek Dereń ^{1,*}

¹ Institute of Low Temperature and Structure Research, Polish Academy of Sciences, ul. Okólna 2, 50-422 Wrocław, Poland; o.bezkrovna@intibs.pl (O.B.); r.lisiecki@intibs.pl (R.L.); b.macalik@intibs.pl (B.M.)
² Institute for Single Crystals, NAS of Ukraine, Nauky Ave. 60, 61001 Kharkiv, Ukraine
* Correspondence: p.deren@intibs.pl; Tel.: +48-713954178

Abstract: The application of ultraviolet-C light in the field of surface treatment or photodynamic therapy is highly prospective. In this regard, the stable fluorescent silicate SrO-CaO-MgO-SiO₂-Pr₂O₃ glasses able to effectively convert visible excitation on the ultraviolet praseodymium emission were fabricated and examined. An unusual wide-range visible-to-UVC up-conversion within 240–410 nm has been achieved in Pr³⁺-doped glasses, revealing their potential advantage in different sophisticated disinfection technologies. The integrated emission intensity was studied as a function of light excitation power to assess a mechanism attributed to UVC luminescence. Especially, it was revealed that the multicomponent silicate glass qualities and praseodymium ³P_J excited state peculiarities are favorable to obtaining useful broadband ultraviolet up-converted luminescence. The glass dispersion qualities were determined between 450–2300 nm. The impact of praseodymium concentration on Vis-NIR spectroscopic glass qualities was evaluated employing absorption spectra, emission spectra, and decay curves of luminescence associated with two involved praseodymium excited states. Especially, efficient interionic interactions can be inferred by investigating the decrease in ¹D₂ state experimental lifetime in the heavily doped samples. Examination of absorption spectra as a function of temperature implied that excitation at 445 nm should be quite effective up to T = 625 K. Contrary to this, temperature elevation gives rise to a moderate lowering of the visible praseodymium luminescence.

Keywords: optical glasses; UVC up-conversion; Pr luminescence



Citation: Bezkravna, O.; Lisiecki, R.; Macalik, B.; Dereń, P.J. UVC Up-Conversion and Vis-NIR Luminescence Examined in SrO-CaO-MgO-SiO₂ Glasses Doped with Pr³⁺. *Materials* **2024**, *17*, 1771. <https://doi.org/10.3390/ma17081771>

Academic Editors: Francesco Baino and Maziar Montazerian

Received: 15 March 2024

Revised: 8 April 2024

Accepted: 8 April 2024

Published: 12 April 2024



Copyright: © 2024 by the authors. Licensee MDPI, Basel, Switzerland. This article is an open access article distributed under the terms and conditions of the Creative Commons Attribution (CC BY) license (<https://creativecommons.org/licenses/by/4.0/>).

1. Introduction

Many diseases are transmitted by airborne droplets and contact surfaces on which viruses, streptococci, staphylococci, and other microbes settle. This problem becomes particularly relevant during pandemics, the latest being the COVID-19 coronavirus. There is a known method for treating surfaces using ultraviolet lamps; however, they are dangerous for the health of people and animals. The significance of creating stable materials that emit efficiently in the UV region of the spectrum near 250 nm is due to the need to treat surfaces without the use of ultraviolet lamps [1]. The creation of materials that absorb photons from ambient light or sunlight and are capable of converting them into photons in the bactericidal range (220–280 nm) and their application can lead to a constant reduction in the content of adsorbed microbes. Ceramic powder materials based on fluorides and silicates Lu₇O₆F₉:Pr³⁺ and Y₂SiO₅:Pr³⁺ are described in [2], as well as UV-resistant phosphors such as Ca₂Al₂SiO₇:Pr³⁺ [3], which can be used to create such self-sterilizing surfaces.

In [4], a detailed analysis of saturation effects occurred in various fields of nonlinear optics and considered the nonlinear optical properties of various optical materials with a fast nonlinear optical response, which can be promising candidates for photonic applications, such as optical communications, optical limiters, optical data storage, information processing, passive laser mode-locking, etc. In [5], several multiphoton active materials

and major applications of multiphoton excitation were described, including pumped lasing to achieve tunable up-conversion of coherent light.

In addition, recently more and more attention has been paid to the creation of light-emitting diodes as efficient, energy-saving, and environmentally friendly semiconductor lighting. Fluorescent glasses are expected to replace phosphors for LEDs since they have advantages over conventional phosphors [6], such as uniform light emission, lower manufacturing costs, and better thermal stability.

Pr^{3+} ions are recognized as effective luminescent activators over a wide range of wavelengths. For UV radiation, Pr^{3+} ions have an advantage due to the corresponding scheme of energy levels and the characteristic $4f^2 \rightarrow 4f^15d^1$ radiation observed in a wide UV range, including UV-C (200–280 nm) [3]. Praseodymium ions are the most effective lanthanides for converting the visible spectrum into UVC due to their qualities, such as a relatively wide range of two-photon excitation, an energetically wide cluster of intermediate states, and the tendency of electrons at excitation in the 4f5d band to relaxation due to high-energy transitions favoring UV radiation [2]. Pr^{3+} ions can emit in the UV range when excited at the 4f5d level directly or through up-conversion (UC) mechanisms [7]. Visible-to-UV conversion of Pr^{3+} ions occurs due to the absorption of blue or violet light (430–490 nm) through $^3\text{H}_4 \rightarrow ^3\text{P}_j$ transitions, followed by the UC of the excitation energy in one Pr^{3+} ion through Excited State Absorption (ESA) or involving two Pr^{3+} ions Energy Transfer Up-conversion (ETU) [2,7]. In addition, Pr^{3+} ions as activators can produce greenish-blue or red emissions due to their excited energy levels $^3\text{P}_0$ or $^1\text{D}_2$ [8].

Visible UV up-conversion using Pr^{3+} -doped materials are excellent candidates for self-disinfecting surfaces. For sterilization in the UV region, various durable matrices with introduced ions emitting in the UV region of the spectrum can be used. The role of such matrices can be performed by glass. The beneficial properties of various types of glass determine their use in various fields. The chemical composition of glass, the additive introduced, and the method of its preparation determine its use. Therefore, glass-based materials are used in fiber optics [9], as radioactive waste immobilizers [10], as bioactive materials [11], or glazes [12]. Due to all the above qualities, Pr^{3+} ions are preferable for introducing them into a stable matrix.

To introduce Pr^{3+} ions, we chose a glass-based SrO-CaO-MgO-SiO₂ matrix. A few glasses of similar composition are known. The production of (40–62%)SiO₂-(2–15%)ZrO₂-(20–50%)SrO-(4–22.5%)MgO (wt%) glasses was studied in [13], and it was found that compositions with 50 wt.% silica base contributes to the production of the transparent glasses. The authors showed that the introduction of Mg²⁺ ions increased the chemical resistance of glasses when they were treated with alkalis. As shown in [14], alkaline earth metal ions (calcium, barium, strontium, and other ions) dissolve in the Si–O–Si glass phase and, accordingly, can be a substitute for potassium ions in the glass composition of SiO₂-MgO-Al₂O₃-B₂O₃-MgF₂-K₂O-Li₂O-AlPO₄. The composition of bioactive glasses based on the system of 42%SiO₂-34%CaO-6%P₂O₅-18-15.5%SrO-(0-2.5%)Al₂O₃ (in mol%) is described in [11]. The authors of this work indicate that Sr²⁺ and Ca²⁺ ions have similar ionic radii (0.94 Å for Ca²⁺ and 1.16 Å for Sr²⁺), and therefore SrO oxide can be replaced by CaO in the glass composition. In [15], xSrO-(45.55-x)CaO-29.44SiO₂-10.28P₂O₅-14.73MgO (x = 0–5 mol %) bioactive compositions were synthesized through the sol-gel route for the growth of hydroxyapatite on the surface of the materials as bioimplants. Examined in [16], 50SiO₂-10Al₂O₃-2MgO-20CaO-15SrO-3BaO-(0.1–1.5)Pr₂O₃ (in mol %) glasses may be used for efficient visible fiber laser operating at 610 nm and 640 nm wavelengths.

Glasses doped with Pr^{3+} ions demonstrate the potential advantages attributed to broad bands in the wide spectral range and broad-band emission due to the disordered local environment of optically active ions. Among oxide glasses, silicate glasses doped with rare earth ions generally have the broadest absorption and emission bands [16], enabling significant tuning of the useful spectral range. In addition, silicate glasses are characterized by mechanical strength and chemical resistance.

In our work, we synthesized glasses based on alkaline earth metal oxides (Sr, Ca, and Mg) and SiO₂ doped with different concentrations of Pr³⁺ ions, and consequently, their structural, physicochemical, and spectroscopic properties, including absorption, UVC up-conversion, and down-conversion, were examined.

2. Materials and Methods

Reagents SrCO₃ (≥99.9%, Sigma-Aldrich, St. Louis, MO, USA), CaCO₃ (99.95%, Thermo Scientific, Waltham, MA, USA), MgO (Reachem, Mississauga, ON, Canada), Pr₂O₃ (99.9%, Chem PUR, Piekary Śląskie, Poland), and nanopowder of SiO₂ (99.5%, 10–20 nm particle size (BET), Aldrich) were used for the synthesis of glasses. Glasses doped with praseodymium ions were prepared with a composition (in mol %) of 14.27 SrO-14.27 CaO-14.27 MgO-57.19 SiO₂-Pr₂O₃ ($x = 0.036, 0.071, 0.179$ mol % Pr₂O₃) (this is equivalent to 0.5; 1.0; 2.5 at.% Pr³⁺, respectively). The choice of active Pr³⁺ ion concentrations in SCMS glasses is determined by a tradeoff between the praseodymium absorption qualities, especially at the excitation wavelength of 445 nm, and the ability to measure the up-conversion spectra of the material in the ultraviolet region as well as an emission in a wide spectral range. The ionic radii of the involved ions are the following: Mg²⁺ (0.66 Å), Ca²⁺ (0.99 Å) [17], (0.94 Å [11]), Pr³⁺ (1.126 Å) [18], and Sr²⁺ (1.260 Å [18]).

Samples were synthesized by the following procedure: First, the prepared components were transferred to a mortar and thoroughly ground. Next, the powder batch in the crucible was heated to 1450 °C for 2 h. The melt was poured into a brass mold. The glasses were characterized by the X-ray diffraction method (X'Pert PRO PANalytical diffractometer, Ashland, VA, USA, non-monochromatic CuK α radiation). The measurements were carried out in the range of 10–100° of 2 θ with a scanning rate of 20 min⁻¹ for 30 min.

The absorption spectra of the glass samples were measured using a UV-Vis-NIR spectrophotometer (Cary 5000, Agilent, 5301 Stevens Creek Blvd, Santa Clara, CA, USA) in the spectral range of 190–2500 nm. The UV-VIS emission and excitation spectra were measured using an FLS1000 fluorescence spectrometer (Edinburgh Instrument, Livingston, UK) with a 450 W xenon lamp as an excitation source and a Hamamatsu 928 photomultiplier. Up-converted luminescence was measured using a 445 nm diode laser and a UG5 filter (Thorlabs, Newton, NJ, USA). To record emission spectra in the UVC range, a VUV McPherson spectrometer equipped with a water-cooled deuterium lamp and a Hamamatsu photomultiplier R955P (Hamamatsu, 430-0852 2-25-7 Ryoke, Nakaku, Japan) were employed as well. The Linkam system was used to study the effect of temperature on the spectral properties of the glasses. Decay curves of Pr³⁺ luminescence were acquired utilizing an experimental set-up consisting of a Surelite Continuum optical parametric oscillator pumped by the third harmonic of a Nd:YAG laser (Amplitude Laser Group, San Jose, CA, USA), a GDM 1000 (Carl Zeiss, Jena, Germany) double grating monochromator, an R3896 Hamamatsu photomultiplier (Hamamatsu, 430-0852 2-25-7 Ryoke, Nakaku, Japan), and a Tektronix MDO-40-54-B-3 Mixed Domain Oscilloscope (Tektronix Inc., Beaverton, OR, USA).

3. Results and Discussion

3.1. XRD Analysis

X-ray diffraction analysis was carried out to study the structure of as-melted glasses. In the diffraction pattern (Figure 1a) of the SCMS:Pr³⁺ glass samples, only two very weak and diffuse peaks with wide halos can be identified (in the range of 2 $\theta = 23$ –35° and 39–47°), confirming the amorphous nature of the sample. This, in turn, makes their interpretation very difficult. Furthermore, the presence of nanocrystalline (several nm in size) inclusions of silicate phases, which may have characteristic peaks in the regions 2 $\theta = 23$ –35° and 39–47°, cannot be completely excluded. The most pronounced peak around 2 $\theta = 28.8^\circ$ is most likely an amorphous halo, which is characteristic of amorphous or highly disordered SiO₂-based structures.

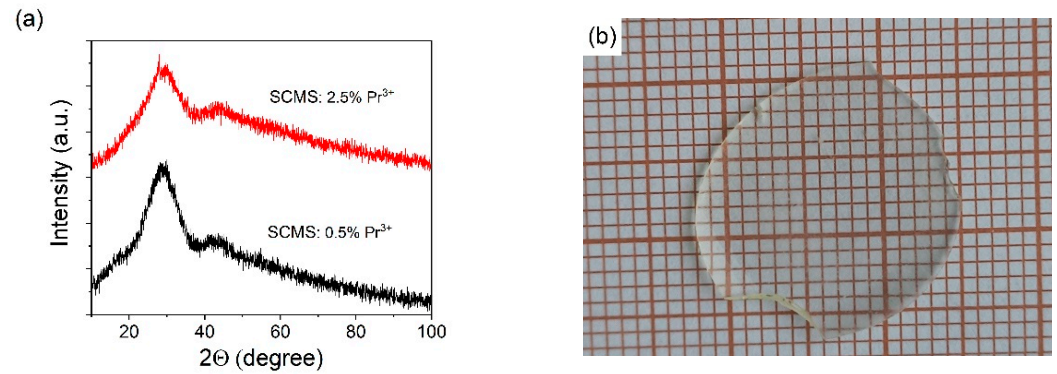


Figure 1. XRD of the SCMS:Pr³⁺ glasses (a), and the photo of the SCMS:1.0% Pr³⁺ glass (b).

An intense peak at 28.81°, as well as less intense peaks in the region $2\theta = 25.99\text{--}26.12^\circ$ and 28.80–29.18°, are characteristic of the SiO₂ crystal structure (ICDS code 96-153-2514). The position of the halo with a maximum near 28.8° is also close to the positions of the peaks of the SiO₂ structure (coesite, ICDS code 96-900-0805), however, high pressure is required for the formation of this structure. Silicates also have peaks in the region of 30–47°.

The structure of CaMgSi₂O₆ (ICSD code 30522) has peaks in the range of 26–31° and in the range of 40–44°. However, CaMgSi₂O₆ does not have the characteristic intense peak near 28.8°, which is characteristic of our glasses and the SiO₂ structures.

The significant blurring of the peak (Figure 1a) with a maximum near 28.8° indicates that the formation of silicate structures (if they occur) is insignificant. Thus, we came to the conclusion that our materials are highly disordered structures based on SiO₂.

3.2. Absorption Spectra, Band Gap, and Refractive Index

Figure 2a shows the absorption spectra of the SCMS glasses doped with Pr³⁺ (0.5, 1.0, and 2.5% Pr³⁺) in the spectral range from 380 nm to 2200 nm. All observed absorption bands are due to electronic transitions from the ³H₄ ground state. The concentration dependence of the absorption coefficient of the ³H₄ → ³P₀ transition of Pr³⁺ ions is linear and is presented in the inset of Figure 2a. As shown in [16], aluminosilicate glasses containing oxides of strontium, calcium, and barium, have no absorption peaks in the wavelength range from 400 nm to 2400 nm. Therefore, all the well-defined peaks observed in Figure 2a are due to the presence of Pr³⁺ ions in the glass samples.

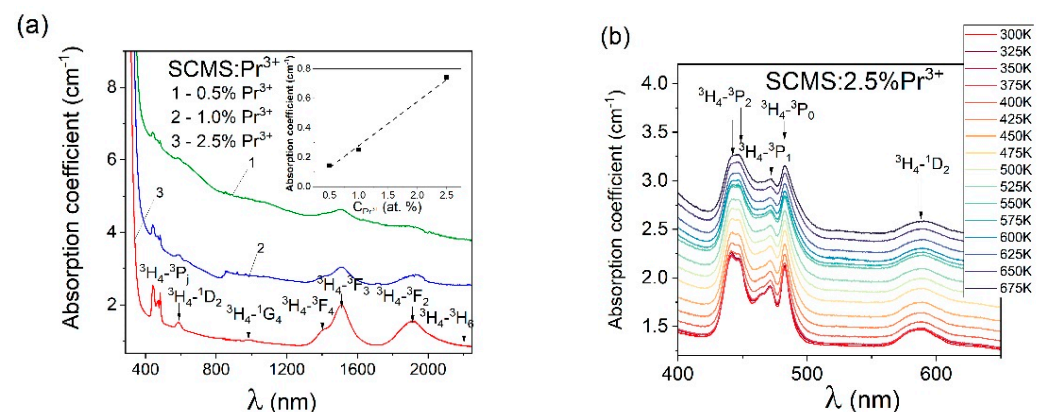


Figure 2. Absorption spectra of SCMS glasses doped with 0.5 (1), 1.0 (2), and 2.5% (3) Pr³⁺ ions (a) (inset shows the dependence of the absorption coefficient of ³H₄ → ³P₀ transition from Pr³⁺ concentration); effect of the temperature on SCMS:2.5% Pr³⁺ absorption bands (b).

After doping the glasses with Pr³⁺ ions, as shown in Figure 2a,b, absorption peaks are located at 441 and 447 nm (³H₄ → ³P₂ transition), 463 (³H₄ → ¹I₆), 471 nm (³H₄ → ³P₁), 482 nm (³H₄ → ³P₀), 586 nm (³H₄ → ¹D₂), 980 nm (³H₄ → ¹G₄), 1397 nm (³H₄ → ³F₄), 1508 nm

($^3\text{H}_4 \rightarrow ^3\text{F}_3$), 1904 nm ($^3\text{H}_4 \rightarrow ^3\text{F}_2$) and near 2200 nm ($^3\text{H}_4 \rightarrow ^3\text{H}_6$). These energy transitions are shown in the energy level diagram of the SCMS:2.5%Pr $^{3+}$ glass shown in Figure 3.

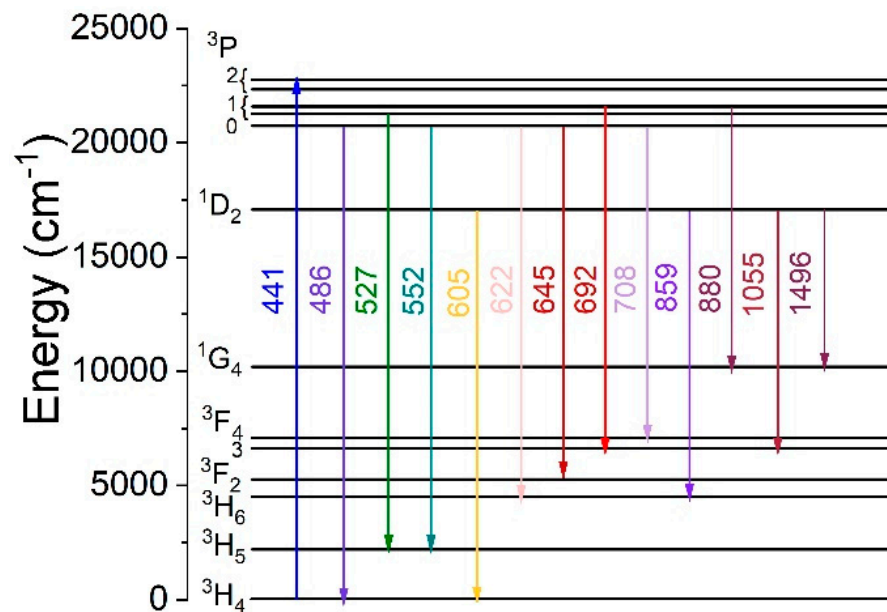


Figure 3. Energy levels scheme of Pr $^{3+}$ ions in SCMS glasses.

In this case, it is worth noticing that the absorption band maxima corresponding to the transitions from the ground state $^3\text{H}_4$ to the excited states $^3\text{P}_j$ were close to those recorded in [16]. On the other hand, the absorption transitions terminated on $^1\text{D}_2$, $^3\text{F}_4$, $^3\text{F}_3$, and $^3\text{H}_6$ Pr $^{3+}$ excited states are slightly shifted to the bands described in [16]. It is the result of the different compositions of the compared silicate glass materials. The relevant aspect of this paper is related to UVC up-converted luminescence, which is excited at 445 nm. Since the used semiconductor excitation source provides quite a high-power density to the glass sample, the impact of higher temperatures on the involved praseodymium absorption bands is worth investigating. In relation, the praseodymium absorption bands attributed to $^3\text{H}_4 \rightarrow ^3\text{P}_j$ and $^3\text{H}_4 \rightarrow ^1\text{D}_2$ transitions for the SCMS:2.5% Pr $^{3+}$ glass were examined as a function of temperature between 300 K and 675 K, i.e., from 26.85 °C to 401.85 °C. Our findings indicate that the examined absorption bands are rather ineffectively broadened at elevated temperatures. Furthermore, the effect of temperature on the $^3\text{H}_4 \rightarrow ^3\text{P}_2$ absorption band is moderate up to $T = 675$ K, and consequently, the excitation of up-converted praseodymium emission at 445 nm should be efficient even at high powers of the laser diode. The thermal-broadening effect and slight decrease in the absorption coefficient may be perceived for the $^3\text{H}_4 \rightarrow ^1\text{D}_2$ absorption band at 586 nm as well.

The optical band gap of SCMS:Pr $^{3+}$ glass was calculated employing Equation (1), as it was presented in [19–21]:

$$(\alpha h\nu)^2 = A(h\nu - E_g), \quad (1)$$

where A —is a constant, h —is Planck's constant, and ν —is the optical frequency. The optical band gap of 4.41 eV was obtained for the SCMS:0.5%Pr $^{3+}$ glass. The refractive index (n) was calculated using Fresnel equations [22]. The optical band gap calculated for the SCMS:0.5%Pr $^{3+}$ glass is close to the values of 4.44–4.50 eV obtained in [22] for TiO₂-SiO₂ mixed thin films.

Figure 4 shows the measured refractive index (n) of SCMS:2.5% Pr $^{3+}$ glass as a function of the incident wavelengths. The dispersive qualities of our silicate glass were examined at wide wavelengths ranging from near-infrared to UV. Concerning that, the value of the refractive index is lowered with the wavelength increasing to 1.56 at 2400 nm. For comparison, the comparable findings were described in [23] for the borosilicate glasses.

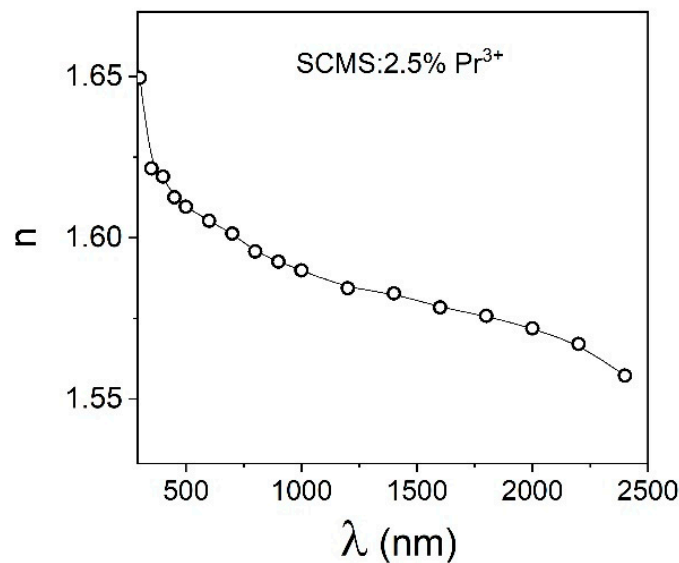


Figure 4. The dependence of the refractive indices of the SCMS:2.5% Pr³⁺ glass from the wavelengths.

3.3. Up-Conversion Phenomena

We obtained up-conversion luminescent radiation in the ultraviolet region in the SCMS:Pr³⁺ glass upon excitations with lower-frequency radiation. As shown in Figure 5, the up-converted luminescence spectrum of Pr³⁺-doped SCMS glass contains a broad band in the 230–330 UV spectral region. The maximum of the up-converted luminescence of the SCMS:Pr³⁺ glass under the 445 nm excitation is located at 275 nm.

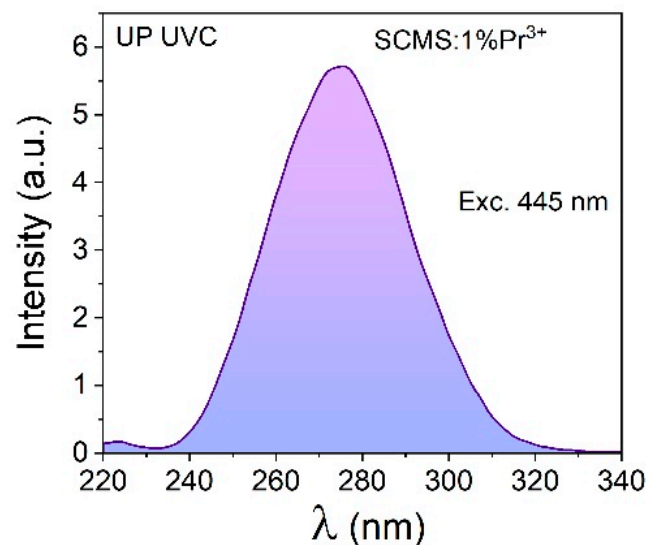


Figure 5. The up-converted UV luminescence of SCMS:1%Pr³⁺ glass excited at 445 nm.

To obtain more insight into the excitation mechanism of the praseodymium UV up-converted emission in the studied silicate glasses, the impact of the incident laser beam power on the integrated anti-Stokes emission was investigated. The result presented in Figure 6 shows the dependence of the up-converted ultraviolet emission on the 445 nm laser diode excitation power. The plot can very well be approximated by a straight line, and it shows that the excitation power is too low to induce the saturation effect. The slopes of the line indicate that the two-photon excitation process is responsible for up-converted emission in the SCMS:Pr³⁺ silicate glass.

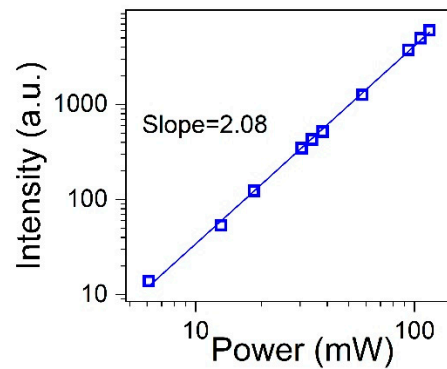


Figure 6. Integrated emission intensities vs. 445 nm CW excitation power for the SCMS:1%Pr³⁺ glass.

The accomplishment of the ultraviolet anti-Stokes praseodymium emission in the studied silicate glasses was confirmed by employing an alternative experimental setup based on an FLS1000 spectrofluorometer.

In contrast to previously described spectra, the currently used detector allows for measuring the up-converted Pr³⁺ emission at longer wavelengths up to 410 nm. On the other hand, its sensitivity is significantly reduced at a higher-energy spectral range. For that, additional broad-band up-converted emission was observed within the 320–410 nm region, and these are presented in Figure 7. The intense emission band is peaked at 392 nm and the weaker UV band is centered at 360 nm. The origin of these bands is explained in the next chapter which describes the excitation and down-converted spectra.

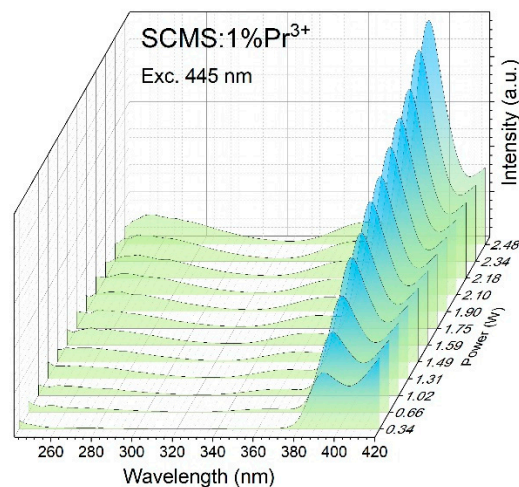


Figure 7. The anti-Stokes UV emission of Pr³⁺-doped SCMS glass excited at several excitation powers up to 2.48 W.

It is recognized that praseodymium ions emit in the UV region of the spectrum in various hosts, including silicate ones. In fact, in [24], authors display that Pr³⁺ ions in LaBSiO₅ powders reveal an intense luminescence band in the 220–280 nm region with a maximum near 231 nm. Xinchun Wang et al. documented up-converted Pr³⁺ luminescence in the UV-350 nm region in the Y₂SiO₅:Pr³⁺ crystal upon excitation by an infrared femtosecond laser at 800 nm [25]. The YSO:Pr host was investigated by E.L. Cates et al. [2], and as a result, the up-conversion spectrum was between 265–360 nm with a maximum of 278 nm under 447 nm excitation. Quite recently, for the other silicate crystal Y₂Si₂O₇:Pr³⁺ [26], two ultraviolet broad bands ranging between ~250 nm to ~390 nm with maximum intensity at 278 nm and 308 nm were achieved under excitation at 445 nm. According to the author's explanation, this resulting anti-Stokes UV praseodymium emission is a consequence of the sequential absorption of two blue photons, as confirmed by the measurements of excitation power dependence.

It is worth noticing that values of the energy gap $E_g = 4.82$ eV and 4.78 eV were reported for Y_2SiO_5 and $Y_2Si_2O_7$ silicates, respectively [27]. These are slightly higher than $E_g = 4.41$ eV estimated for our SCMS glass. It can be concluded that during the effective excitation process at 445 nm, the 3P_J multiplets of Pr^{3+} ions are populated, after which, due to the UC process, the levels of the $4f^{15}d^1$ electronic configuration are fed, and as a result, UV anti-Stokes $4f^{15}d^1 \rightarrow ^3H_J$ emission is observed.

3.4. Excitation and Down-Converted Luminescence Spectra

The optical properties of Pr^{3+} ions were studied in the UV, visible, and near-IR regions. The luminescence excitation spectra of SCMS glasses monitored at 605 nm and 730 nm are presented in Figure 8a,b. As can be seen in the 425–500 nm wavelength range, three peaks are noticeable at 441, 471, and 486 nm, caused by $^3H_4 \rightarrow ^3P_2$, $^3H_4 \rightarrow ^3P_1$, and $^3H_4 \rightarrow ^3P_0$ transitions, respectively. These peaks are close to those presented in [6] for oxyfluoride silicate glasses doped with Pr^{3+} ions (~443, 468, and 481 nm—transitions from the ground state 3H_4 to excited states 3P_2 , 3P_1 , and 3P_0 manifolds, respectively). It can be discerned that the spectral characteristic of the praseodymium excitation band is not affected by the concentration of Pr^{3+} ions in the material under study. In addition, as shown in Figure 8b, the luminescence excitation spectra of glasses contain a broad band in the UV region with a maximum at 273 nm related to $^3H_J-4f^{15}d^1$ inter-configurational transitions of praseodymium. This band is especially intense for the SCMS:2.5% Pr^{3+} glass with a high concentration of dopant.

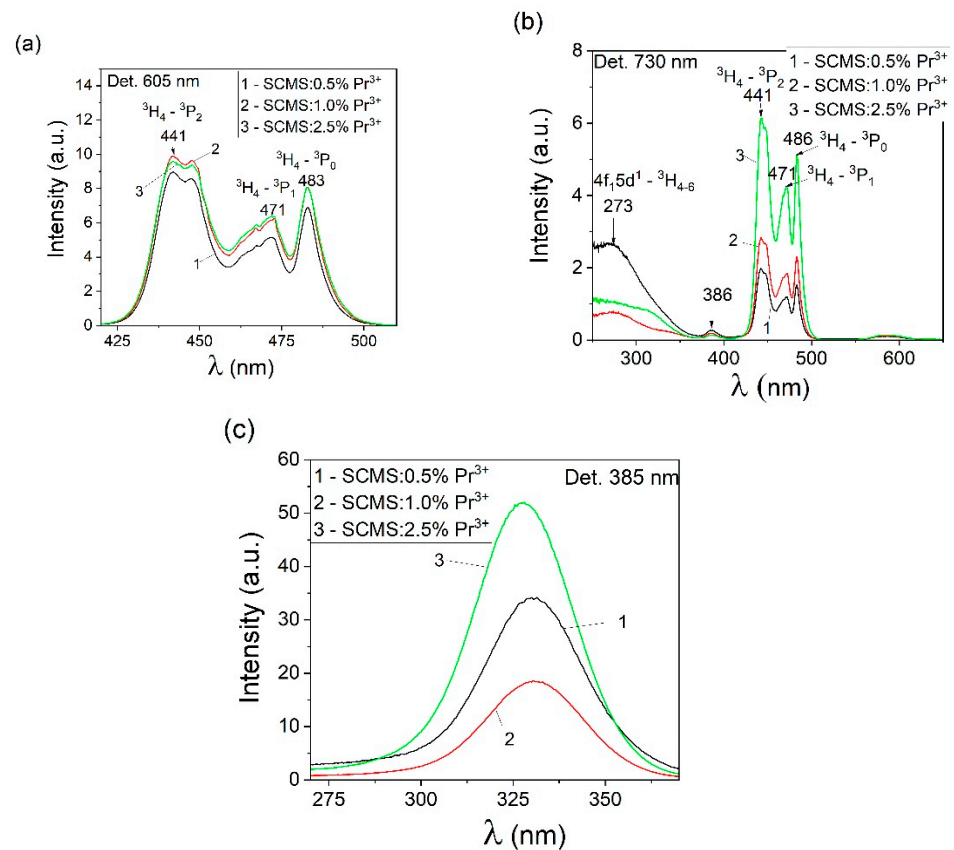


Figure 8. Luminescence excitation spectra of the SCMS: Pr^{3+} glasses with different concentrations of Pr^{3+} ions (1—0.5%, 2—1.0%, 3—2.5%) detected at 605 nm (a), 730 nm (b), and 385 nm (c).

An additional peak of the luminescence excitation band at 386 nm was observed for all SCMS glass samples. In [8], an additional peak with a maximum at 355 nm was also observed for the luminescence excitation spectra of $La_2Zr_2O_7:Pr^{3+}$ nanophosphors, and the

authors associated the appearance of this peak with the intrinsic defect absorption or the virtual charge transfer of Pr^{3+} ions.

The appearance of a band with a maximum of 330 nm is characteristic of the luminescence excitation spectra of our glasses when detected at 385 nm (Figure 8c). When excited into this band at 335 nm, an intense luminescence band is observed (Figure 9c) with a maximum near 400 nm. A similar luminescence band was studied in [28] for the porous SiO_2 matrix. The authors of this work showed that when the pure SiO_2 matrix was excited at 335 nm, a broad luminescence band with a maximum at 380 nm (at room temperature) was observed and suggested that the nature of this band could be due to either isolated silanol groups or OH-related centers. However, during the synthesis of our glass, tetraethoxysilane was not used. We carried out the synthesis at high temperatures, so the more likely appearance of this band is associated with the presence of defects in the examined SCMS glasses.

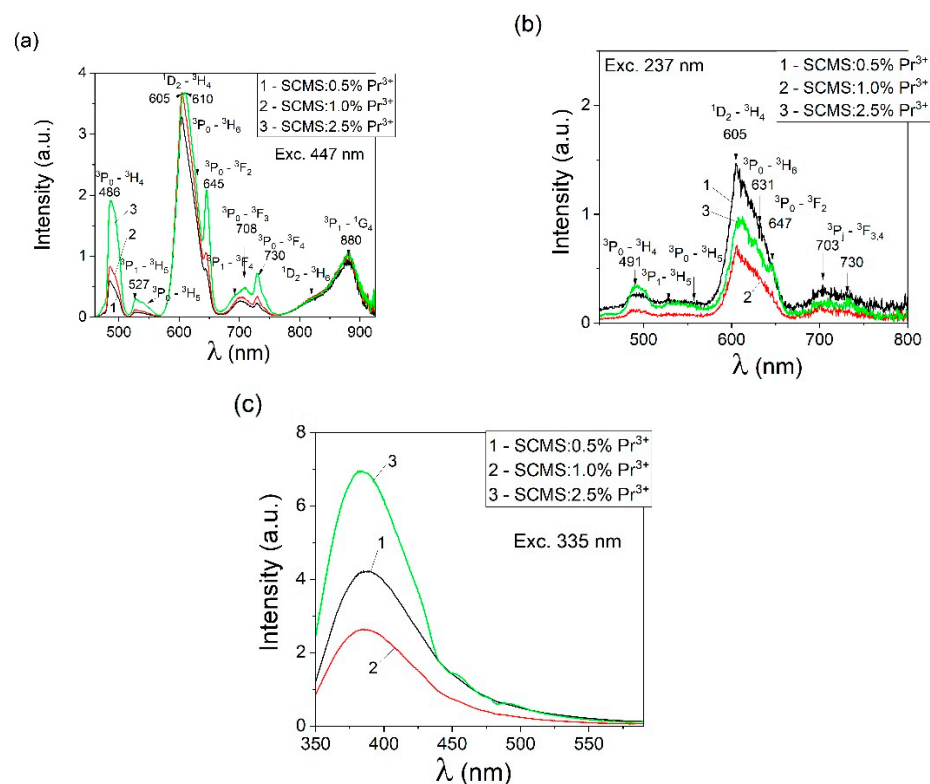


Figure 9. Luminescence spectra of the SCMS: Pr^{3+} glasses with the different concentrations of Pr^{3+} ions (0.5% (1), 1.0% (2), and 2.5% (3)) excited at 447 nm (a), 227 nm (b), and 335 nm (c).

In [29], it was stated that silicate glasses obtained in a reducing atmosphere (H_2/He) can have a luminescence band with a maximum at 3.1 eV (400 nm) (strong) and 4.2 eV (295 nm) (very weak) with excitation at 5.17 eV (240 nm). The authors stated that such bands are also characteristic of studies in an oxidizing atmosphere. This band is identified as a Si-related center, which was assigned to Si(II), dissolved in the silica network.

It can be assumed that the presence of a band with a maximum at 400 nm in our glasses can also be due to the formation of chains of two-fold coordinated Si atoms with two oxygen neighbors; moreover, the presence of oxygen vacancies is also possible.

The luminescence spectra of the SCMS: Pr^{3+} glasses were measured in the visible and near-infrared regions. Samples of the SCMS glasses doped with Pr^{3+} were excited into absorption bands at 237 nm and 447 nm. The luminescence spectra of the doped glasses are presented in Figure 9a,b. The involved transitions are shown as the solid arrows in the energy level scheme of Pr^{3+} ions in the SCMS glasses (Figure 3).

When praseodymium luminescence is excited at 447 nm (Figure 9a), the emission bands appear with a maximum at 486 nm ($^3P_0 \rightarrow ^3H_4$), 527 nm ($^3P_1 \rightarrow ^3H_5$), and 552 nm ($^3P_0 \rightarrow ^3H_5$). The most intense band with a maximum at 605 nm ($^1D_2 \rightarrow ^3H_4$) contains weaker components near 631 nm ($^3P_0 \rightarrow ^3H_6$) and at 645 nm ($^3P_0 \rightarrow ^3F_2$). The remaining maxima can be discerned at 692 nm ($^3P_1 \rightarrow ^3F_4$), 708 nm ($^3P_0 \rightarrow ^3F_3$), 730 nm ($^3P_0 \rightarrow ^3F_4$), 880 nm ($^3P_1 \rightarrow ^1G_4$), and at 823 nm ($^1D_2 \rightarrow ^3H_6$).

Figure 9b shows the luminescence spectrum excited at 237 nm, and consequently, the emission bands appear with maxima near 491 nm ($^3P_0 \rightarrow ^3H_4$), 533 nm ($^3P_1 \rightarrow ^3H_5$), 556 nm ($^3P_0 \rightarrow ^3H_5$), the most intense 605 nm ($^1D_2 \rightarrow ^3H_4$), with shoulder maxima at 631 nm ($^3P_0 \rightarrow ^3H_6$), and 647 nm ($^3P_0 \rightarrow ^3F_2$), as well as a band with a small maximum at 703 nm and 736 nm ($^3P_1 \rightarrow ^3F_{3,4}$). Eventually, it can be perceived that in the visible luminescence spectra of the SCMS:Pr³⁺ glasses, red emission is prominent at ~605 nm ($^1D_2 \rightarrow ^3H_4$ transition). The comparable branching ratio of praseodymium luminescence and the location of the examined peaks were documented in [30] for Pr³⁺-doped calcium aluminosilicate glasses. Moreover, the emission peaks of Pr³⁺ ions observed in our SCMS glasses coincide with the emission peaks reported in [6] for SiO₂-Al₂O₃-CaO-CaF₂-TiO₂: Pr₂O₃ glasses excited at 443 nm.

It should be noted that when the glass samples are excited at 237, the maximum luminescence intensity of the $^1D_2 \rightarrow ^3H_4$ transition (605 nm) decreases for the SCMS:1% Pr³⁺ and SCMS:2.5% Pr³⁺ samples by a factor of 1.5–2 in relation to a glass with a low concentration of Pr³⁺ ions.

The decrease in praseodymium luminescence intensity related to the $^1D_2 \rightarrow ^3H_4$ transition near 605 nm with increasing dopant concentration may be due to cross-relaxation phenomena taking place between two neighboring optically active ions. As can be seen from Figure 9a, the ratio of peak intensities at 484 nm relative to the peak intensity at 605 nm is 0.18, 0.23, and 0.51, with an increase in Pr³⁺ ion concentration from 0.5 to 1.0, and 2.5%, respectively. Our findings indicated that visible emission of praseodymium in the SCMS glasses can be efficiently excited employing excitation bands at 441, 471, and 486 nm corresponding to $^3H_4 \rightarrow ^3P_2$, $^3H_4 \rightarrow ^3P_1$, and $^3H_4 \rightarrow ^3P_0$ transitions, and a higher-energy UV excitation is useful as well.

The luminescence of SCMS glass doped with 1% Pr³⁺ measured in the near-infrared wavelength range of 800–1700 nm with excitation at 447 nm is displayed in Figure 10. The NIR emission spectra consist of three bands that may be assigned to $^3P_1 \rightarrow ^1G_4$ (888 nm), $^1D_2 \rightarrow ^3F_4$ (1055 nm), and $^1D_2 \rightarrow ^1G_4$ (1496 nm) transitions. The band centered at 1055 nm is the most intense, and a transition terminated on the 1G_4 level covers a wider 1300–1630 spectral range.

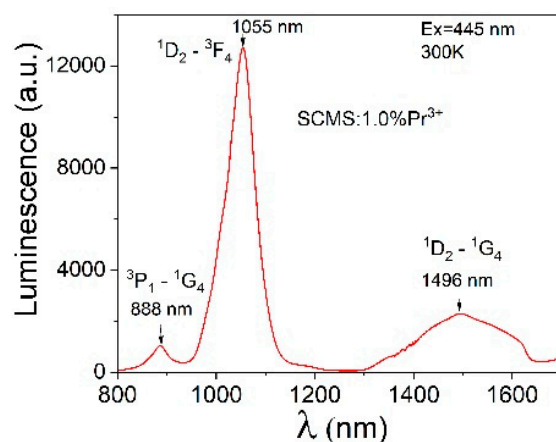


Figure 10. Near-infrared luminescence of the SCMS:1% Pr³⁺ glass.

3.5. Impact of Temperature on Excitation and Luminescence Spectra

A study on the effect of 85 K (−188/15 °C)–715 K (441.85 °C) temperature on the luminescence excitation spectra of the SCMS:1% Pr³⁺ glass (³H₄–³P_J transitions) has been prepared, and the resulting spectra are presented in Figure 11a. At higher temperatures, the higher-energy crystal field components of praseodymium ground state ³H₄ are more effectively populated, consequently, the consecutive transitions to the involved sublevels of ³P_J multiplets take place. This effect, combined with the inherent thermal line shift and broadening, gives rise to the emission band extension, especially at longer wavelengths. In contrast to that, overall band intensity is reduced with temperature increasing. Particularly, at low temperatures, two high-energy components at 441 and 447 nm are more pronounced and become efficiently depressed at higher temperatures.

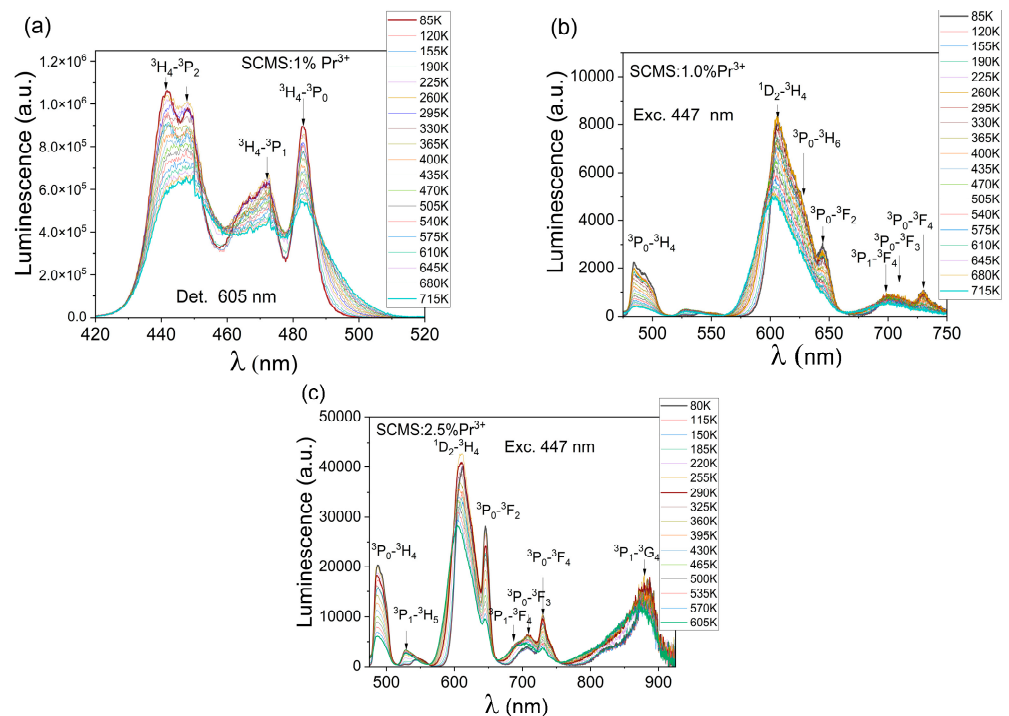


Figure 11. Luminescence excitation spectra of the SCMS:1% Pr³⁺ glass, $\lambda_{\text{det}} = 605$ nm (a) and luminescence spectra of the SCMS:1% Pr³⁺ (b) and SCMS:2.5% Pr³⁺ (c) glasses excited at 447 nm measured in a wide temperature range.

The praseodymium luminescence originating in ³P_J and ¹D₂ multiplets was measured as a function of temperature 85 K (−188/15 °C)–715 K (441.85 °C) for the SCMS glass doped with 1% Pr³⁺, and the adequate spectra are presented in Figure 11b. The most intense band at 605 nm is effectively broadened within shorter wavelengths, and the peak maximum is blue-shifted as well. It is a consequence of the population of higher-energy crystal field sublevels attributed to the involved praseodymium luminescent excited states.

We investigated the variation of luminescence intensity ratio (LIR) related to (³P₀–³H₄/³P₁–³H₅) praseodymium transitions as a function of 85–715 K temperature to evaluate the suitability of the studied materials for applications in optical sensing thermometry. The impact of temperature on the determined luminescence intensity ratio was used to estimate the corresponding absolute (S_A) and relative (S_R) thermal sensitivities for SCMS:1%Pr and SCMS:2.5%Pr glasses. The achieved results are depicted in Figure 12a–d. The luminescence intensity ratio was fitted according to the relation:

$$\text{LIR}(T) = A + B \exp(\Delta E / (k_B T)) \quad (2)$$

where ΔE is the energy difference between the thermalized $^3P_{0,1}$ levels, k_B is the Boltzmann constant, T is the temperature expressed in absolute scale [K] and A and B are constants.

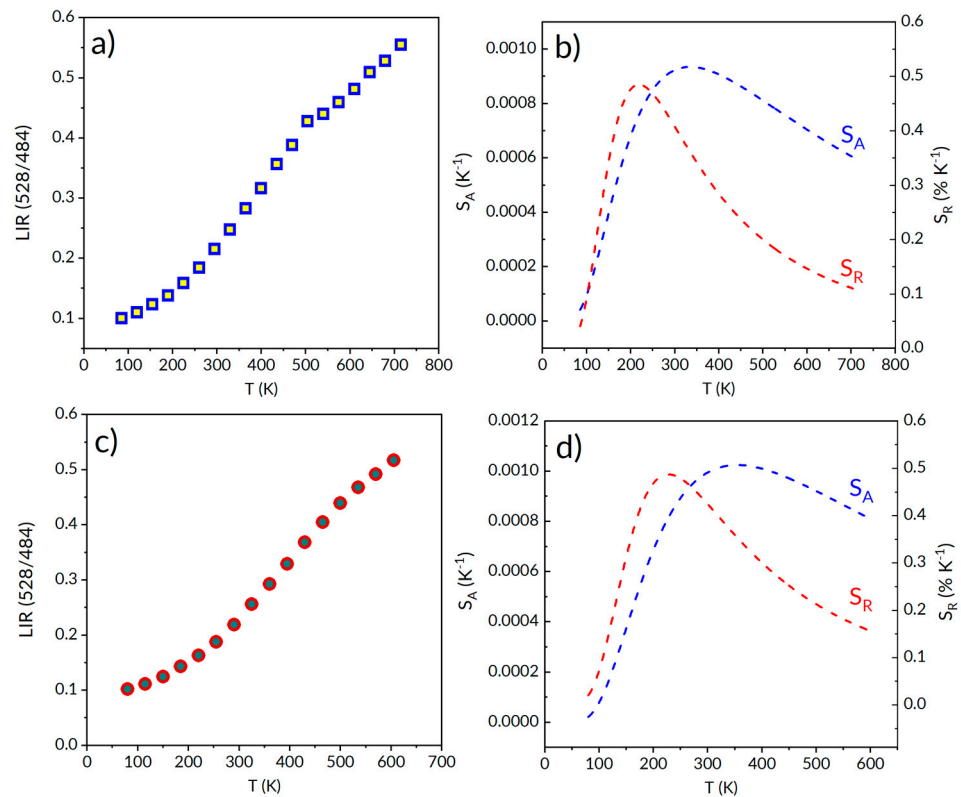


Figure 12. Luminescence intensity ratios correspond to praseodymium luminescence (a) of SMCS:1%Pr³⁺ (a,b) and SMCS:2.5%Pr³⁺ (c,d) glasses, as well as the corresponding absolute and relative thermal sensitivities estimated for LIR (527/486).

Luminescence intensity ratios LIR (527/486) increase exponentially with temperature elevation, and the maximum absolute temperature sensitivity is reached for $T = 223$ K and $T = 230$ K, and amount to $8.71 \times 10^{-4} \text{ K}^{-1}$ and $9.83 \times 10^{-4} \text{ K}^{-1}$ for SCMS:1%Pr³⁺ and SCMS:2.5%Pr³⁺ respectively.

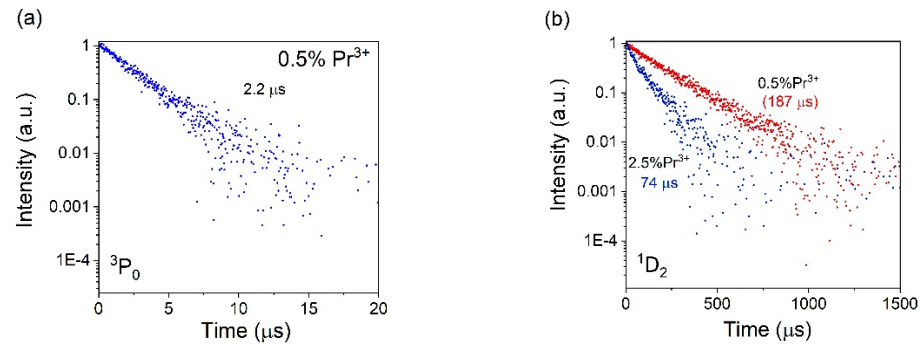
The highest values of relative sensitivity, $S_R = 0.52\% \text{ K}^{-1}$ at $T = 330$ K and $S_R = 0.48\% \text{ K}^{-1}$ at $T = 322$ K, were found for SCMS:1%Pr³⁺ and SCMS:2.5%Pr³⁺ glasses, respectively. Concerning that, our glasses can be considered a potential luminescent optical temperature sensor, applying thermally coupled levels of praseodymium. Quite recently, a maximum relative sensitivity of $1.0\% \text{ K}^{-1}$ has been reported for Pr³⁺/Yb³⁺ co-doped fluoride phosphate glass [31]. This estimated sensitivity is higher in relation to SCMS:Pr³⁺ glass, regardless of our optical systems can be useful at extended temperature ranges up to 715 K.

3.6. Relaxation Dynamic of Pr³⁺ Excited States

Luminescence decay curves were measured for 3P_0 and 1D_2 excited states at 495 nm or 605 nm under excitation at 447 nm. As can be seen from Table 1 and Figure 13a, the experimental lifetime of the 3P_0 excited state changes slightly with increasing dopant concentration in the studied glass. In fact, an increase in the concentration of Pr³⁺ ions from 0.5% to 2.5% leads to an insignificant decrease in average lifetime $\tau_{exp.}$ of 3P_0 levels from 2.20 μs to 2.06 μs .

Table 1. Experimental lifetimes of 3P_0 and 1D_2 levels of Pr^{3+} in SCMS glasses.

SCMS:Pr ³⁺ Glasses	τ	
	3P_0 [μ s]	1D_2 [μ s]
0.5% Pr ³⁺	2.20	187
1.0% Pr ³⁺	2.12	145
2.5% Pr ³⁺	2.06	74

**Figure 13.** Photoluminescence decay profiles of 3P_0 (a) and 1D_2 (b) levels upon observation at 495 or 605 nm of Pr^{3+} -doped SCMS glasses.

A different effect is recognized for 1D_2 levels of Pr^{3+} -doped SCMS (Table 1 and Figure 13b). An increase in the concentration of Pr^{3+} ions leads to a considerable decrease in τ_{exp} . (from 187 μ s to 74 μ s at a concentration of Pr^{3+} ions of 0.5 and 2.5%, respectively). Our findings indicate that the efficiency of Pr-Pr energy transfer can be found to be around 60% in SCMS glasses.

To examine the interaction between optically active ions in SCMS:Pr³⁺ glasses, the Inokuti–Hirayama model has been utilized [32]. When the effectiveness of interionic energy transfer is more significant in relation to the time evolution of praseodymium, luminescence intensity can be described as:

$$\Phi(t) = A \exp \left[- \left(\frac{t}{\tau_0} \right) - \alpha \left(\frac{t}{\tau_0} \right)^{3/S} \right] \quad (3)$$

where A is constant, $\Phi(t)$ denotes the emission intensity after pulse excitation, $S = 6$ for dipole-dipole interactions, τ_0 defines the intrinsic decay probability of the donor involved excited state when the acceptor is absent; furthermore, α is the parameter expressed as:

$$\alpha = \left(\frac{4}{3\pi} \right) \Gamma \left(1 - \frac{3}{S} \right) N_a R_0^3 \quad (4)$$

where R_0 is the critical ion-ion energy transfer distance, N_a is the acceptor concentration $\Gamma = 1.77$ (for $S = 6$) is Euler's function. The nonexponential decay curve recorded for 1D_2 luminescence in heavily doped SCMS:2.5%Pr³⁺ glass was applied to estimate energy transfer quality. In relation to that, the α parameter was fitted to be 1.9 and the critical energy transfer distance R_0 is equal to 8.9 Å for the studied glass host. Employing the relations $C_{da} = R_0^6 \tau_0^{-1}$ and $W_{da} = C_{da} R_0^{-6}$ the energy transfer parameter corresponds to the value of $2.40 \times 10^{-39} \text{ cm}^6 \text{ s}^{-1}$ and a donor-acceptor energy transfer rate is estimated to be $5 \times 10^6 \text{ s}^{-1}$. The estimated critical distance R_0 is higher than 5 Å, hence the applied IH model validates the contribution of multipolar Pr-Pr interactions in the material under study [33]. For the comparison, the energy transfer parameters $C_{da} = 6.39 \times 10^{-43} \text{ cm}^6 \text{ s}^{-1}$ and $W_{da} = 13 \times 10^6 \text{ s}^{-1}$ were estimated for Pr-doped multi-component silicate photonic films [34]. In relation to our glass, this praseodymium highly-doped silicate optical system is characterized by a significant D-A energy transfer rate and especially dipole-quadrupole

mechanisms leading to significant quenching phenomena. Contrary, for higher Pr_2O_3 concentration in $\text{P}_2\text{O}_5\text{-Na}_2\text{O-Al}_2\text{O}_3\text{-Gd}_2\text{O}_3$ glass [35], particularly the reliable fitting is documented for $S = 6$ and dipole-dipole interaction between optically active ions takes place.

4. Conclusions

In this work, we studied UVC up-conversion phenomena and optical properties of $\text{SrO-CaO-MgO-SiO}_2\text{-Pr}_2\text{O}_3$ glass matrix (0.5–2.5% Pr^{3+}) in UV-vis-near-IR regions. Effective UVC up-converted emission within a wide spectral region was observed when 445 nm excitation into praseodymium $^3\text{P}_1$ multiplets took place. The dependence of the integrated anti-Stokes emission intensity on the laser diode power indicates that the two-photon excitation process is responsible for the population of the involved luminescent levels. The luminescence of Pr^{3+} in the studied glasses mainly corresponds to peaks in blue (486 nm), reddish-orange (605 nm), and near-infrared (1055 nm) regions. The effect of temperature on praseodymium luminescence was examined in SCMS glass up to $T = 715$ K. Accordingly, the luminescence intensity ratio between thermally coupled ($^3\text{P}_0\text{-}^3\text{H}_4/{}^3\text{P}_1\text{-}^3\text{H}_5$) praseodymium excited states was utilized to estimate maximal relative temperature sensitivity, $S_R = 0.52\% \text{ K}^{-1}$ at $T = 330$ K, for SCMS:1% Pr^{3+} glass. The considerable nonradiative energy transfer between praseodymium ions occurs, especially in glasses containing higher concentrations of luminescent ions. Relaxation dynamic study of $^1\text{D}_2$ luminescence made it possible to estimate critical energy transfer distance R_0 , which amounts to 8.9 Å. Eventually, these findings indicate that the synthesized glasses can be suitable as solid-state media for various photonic applications, including the development of UVC self-sterilizing surfaces or temperature optical sensors.

Author Contributions: Conceptualization, O.B. and P.J.D.; Methodology, O.B., R.L. and B.M.; Data curation, O.B., R.L. and B.M.; Writing—original draft, O.B. and R.L.; Writing—review & editing, O.B., R.L. and P.J.D.; Investigation, O.B., R.L. and B.M.; Visualization, O.B., R.L. and B.M.; Supervision, P.J.D.; Project administration, P.J.D. All authors have read and agreed to the published version of the manuscript.

Funding: This work was supported by the National Science Centre, Poland, under grant number DEC-2021/41/B/ST5/03792 entitled: Phosphors for UVC LEDs: Self-Disinfecting Surfaces.

Institutional Review Board Statement: Not applicable.

Informed Consent Statement: Not applicable.

Data Availability Statement: The data presented in this study are openly available in Zenodo at <https://doi.org/10.5281/zenodo.10817241>.

Conflicts of Interest: The authors declare no conflict of interest.

References

1. Eadie, E.; Hiwar, W.L.; Fletcher, L.; Tidswell, E.; O'Mahoney, P.; Buonanno, M.; Welch, D.; Adamson, C.S.; Brenner, D.J.; Noakes, C.; et al. Far-UVC (222 nm) efficiently inactivates an airborne pathogen in a room-sized chamber. *Sci. Rep.* **2022**, *12*, 4373. [[CrossRef](#)]
2. Cates, E.L.; Wilkinson, A.P.; Kim, J.-H. Visible-to-UVC upconversion efficiency and mechanisms of $\text{Lu}_7\text{O}_6\text{F}_9\text{:Pr}^{3+}$ and $\text{Y}_2\text{SiO}_5\text{:Pr}^{3+}$ ceramics. *J. Lumin.* **2015**, *160*, 202–209. [[CrossRef](#)]
3. Nilova, D.; Antuzevics, A.; Krieke, G.; Doke, G.; Pudza, I.; Kuzmin, A. Ultraviolet-C persistent luminescence and defect properties in $\text{Ca}_2\text{Al}_2\text{SiO}_7\text{:Pr}^{3+}$. *J. Lumin.* **2023**, *263*, 120105. [[CrossRef](#)]
4. Rao, A.S. Saturation effects in nonlinear absorption, refraction, and frequency conversion: A review. *Optik* **2022**, *267*, 169638. [[CrossRef](#)]
5. He, G.S.; Tan, L.S.; Zheng, Q.; Prasad, P.N. Multiphoton absorbing materials: Molecular designs, characterizations, and applications. *Chem. Rev.* **2008**, *108*, 1245–1330. [[CrossRef](#)]
6. He, Z.; Zhu, C.; Huang, S.; Wu, X. Luminescent properties of Pr^{3+} and Tm^{3+} doped oxyfluoride silicate glasses for light emitting diode applications. *Vacuum* **2019**, *159*, 269–276. [[CrossRef](#)]
7. Flizikowski, G.A.S.; Zanuto, V.S.; Novatski, A.; Nunes, L.A.O.; Malacarne, L.C.; Baesso, M.L.; Astrath, N.G.C. Upconversion luminescence and hypersensitive transitions of Pr^{3+} -doped calcium aluminosilicate glasses. *J. Lumin.* **2018**, *202*, 27–31. [[CrossRef](#)]

8. Kumar, A.; Manam, J. Observation of up conversion/down conversion luminescence and structural analysis of $\text{La}_2\text{Zr}_2\text{O}_7:\text{Pr}^{3+}$ nano phosphors. *Mater. Sci. Semicond. Proc.* **2022**, *148*, 106828. [[CrossRef](#)]
9. Hao, L.; Xitang, W.; Baoguo, Z.; Zhoufu, W.; Yuhan, Y. Structure and properties of CaO-MgO-SiO₂ inorganic glass fiber with additives (Al₂O₃, Y₂O₃). *J. Wuhan Univ. Technol.-Mat. Sci. Edit.* **2012**, *27*, 58–62. [[CrossRef](#)]
10. Pilania, R.K.; Dube, C.L. Matrices for radioactive waste immobilization: A review. *Front. Mater.* **2023**, *10*, 1236470. [[CrossRef](#)]
11. Tripathi, H.; Rath, C.; Kumar, A.S.; Manna, P.P.; Singh, S.P. Structural, physico-mechanical and in-vitro bioactivity studies on SiO₂-CaO-P₂O₅-SrO-Al₂O₃ bioactive glasses. *Mater. Sci. Eng. C* **2019**, *94*, 279–290. [[CrossRef](#)] [[PubMed](#)]
12. Gajek, M.; Lesniak, M.; Sitarz, M.; Stodolak-Zych, E.; Rapacz-Kmita, A. The crystallization and structure features of glass within the K₂Oe-MgO-CaO-Al₂O₃-SiO₂-(BaO) system. *J. Mol. Struct.* **2020**, *1220*, 128747. [[CrossRef](#)]
13. Karasu, B.; Cable, M. The chemical durability of SrO-MgO-ZrO₂-SiO₂ glasses in strongly alkaline environments. *J. Eur. Ceram. Soc.* **2000**, *20*, 2499–2508. [[CrossRef](#)]
14. Garai, M.; Sasmal, N.; Karmakar, B. Effects of M²⁺ (M = Ca, Sr and Ba) addition on crystallization and microstructure of SiO₂-MgO-Al₂O₃-B₂O₃-K₂O-F Glass. *Indian J. Mater. Sci.* **2015**, *2015*, 638341. [[CrossRef](#)]
15. Kaur, P.; Singh, K.J.; Kaur, S.; Kaur, S.; Singh, A.P. Sol-gel derived strontium-doped SiO₂-CaO-MgO-P₂O₅ bioceramics for faster growth of bone like hydroxyapatite and their in vitro study for orthopedic applications. *Mater. Chem. Phys.* **2020**, *245*, 122763. [[CrossRef](#)]
16. Sun, Y.; Yu, F.; Liao, M.; Wang, X.; Li, Y.; Hu, L.; Knight, J. Emission properties of Pr³⁺-doped aluminosilicate glasses at visible wavelengths. *J. Lumin.* **2020**, *220*, 117013. [[CrossRef](#)]
17. Igashira, K.; Nakauchi, D.; Ogawa, T.; Kato, T.; Kawaguchi, N.; Yanagida, T. Effects of dopant concentration in Eu-doped Ca₂MgSi₂O₇ single crystalline scintillators. *Mater. Res. Bull.* **2021**, *135*, 111155. [[CrossRef](#)]
18. Antuzevics, A.; Doke, G.; Kriek, G.; Rodionovs, P.; Nilova, D.; Cirulis, J.; Fedotovs, A.; Rogulis, U. Shortwave Ultraviolet Persistent Luminescence of Sr₂MgSi₂O₇:Pr³⁺. *Materials* **2023**, *16*, 1776. [[CrossRef](#)] [[PubMed](#)]
19. Zhang, J.; Jin, Y.; Wu, H.; Chen, L.; Hu, Y. Giant enhancement of a long afterglow and optically stimulated luminescence phosphor BaCaSiO₄:Eu²⁺ via Pr³⁺ codoping for optical data storage. *J. Lumin.* **2023**, *263*, 119971. [[CrossRef](#)]
20. Dagdale, S.R.; Harde, G.B.; Paturkar, V.G.; Muley, G.G. Synthesis and optical properties of borate glass of system 3Li₂O-2K₂O-5B₂O₃. *Res. J. Chem. Sci.* **2017**, *7*, 30–32.
21. Pratima, B.M.; Valleti, K.; Subrahmanyam, A. Optical and mechanical properties of Sol-gel prepared Titania (TiO₂)-Silica (SiO₂) mixed thin films 'as prepared at 300K' without any post heat treatment. *Mater. Res. Express* **2019**, *6*, 026407. [[CrossRef](#)]
22. McClymer, J.P. Index of refraction measurement using the Fresnel equations. *Rev. Sci. Instrum.* **2014**, *85*, 086107. [[CrossRef](#)]
23. Saddeek, Y.B.; Aly, K.A.; Bashier, S.A. Optical study of lead borosilicate glasses. *Phys. B* **2010**, *405*, 2407–2412. [[CrossRef](#)]
24. Zhou, L.; Zhou, W.; Shi, R.; Liu, C.; Huang, Y.; Tao, Y.; Liang, H. Luminescence and energy transfer of Ce³⁺ and Pr³⁺ in LaBSiO₅. *J. Lumin.* **2016**, *177*, 178–183. [[CrossRef](#)]
25. Wang, X.; Qiu, J.; Song, J.; Xu, J.; Liao, Y.; Sun, H.; Cheng, Y.; Xu, Z. Simultaneous three-photon absorption induced ultraviolet upconversion in Pr³⁺:Y₂SiO₅ crystal by femtosecond laser irradiation. *Opt. Commun.* **2008**, *281*, 299–302. [[CrossRef](#)]
26. Fałat, P.; Tsang, M.Y.; Maliszewska, I.; Zelewski, S.J.; Cichy, B.; Ohulchanskyy, T.Y.; Samoć, M.; Nyk, M.; Wawrzyńczyk, D. Enhanced biocidal activity of Pr³⁺ doped yttrium silicates by Tm³⁺ and Yb³⁺ co-doping. *Mater. Adv.* **2023**, *4*, 5827. [[CrossRef](#)]
27. Ching, W.Y.; Ouyang, L.; Xu, Y.N. Electronic and optical properties of Y₂SiO₅ and Y₂Si₂O₇ with comparisons to α-SiO₂ and Y₂O₃. *Phys. Rev. B* **2003**, *67*, 245108. [[CrossRef](#)]
28. Masalov, A.A.; Seminko, V.V.; Kononets, N.V.; Maksimchuk, P.O.; Bespalova, I.I.; Voloshina, L.I.; Malyukin, Y.V. ZnSe nanocrystals obtained in pores of SiO₂ matrix with temperature stable green luminescence. *J. Lumin.* **2017**, *181*, 334–337. [[CrossRef](#)]
29. Kohketsu, M.; Awazu, K.; Kawazoe, H.; Yamane, M. Photoluminescence Centers in VAD SiO₂ Glasses Sintered under Reducing or Oxidizing Atmospheres. *Jpn. J. Appl. Phys.* **1989**, *28*, 615–621. [[CrossRef](#)]
30. Morassuti, C.Y.; Andrade, L.H.C.; Silva, J.R.; Baesso, M.L.; Guimarães, F.B.; Rohling, J.H.; Nunes, L.A.O.; Boulon, G.; Guyot, Y.; Lima, S.M. Spectroscopic investigation and interest of Pr³⁺-doped calcium aluminosilicate glass. *J. Lumin.* **2019**, *210*, 376–382. [[CrossRef](#)]
31. Maturi, F.E.; Gaddam, A.; Brites, C.D.S.; Souza, J.M.M.; Eckert, H.; Ribeiro, S.J.L.; Carlos, L.D.; Manzan, D. Extending the Palette of Luminescent Primary Thermometers: Yb³⁺/Pr³⁺ Co-Doped Fluoride Phosphate Glasses. *Chem. Mater.* **2023**, *35*, 7229–7238. [[CrossRef](#)]
32. Inokuti, M.; Hirayama, F. Influence of Energy Transfer by the Exchange Mechanism on Donor Luminescence. *J. Chem. Phys.* **1965**, *43*, 1978–1989. [[CrossRef](#)]
33. Iwaki, M.; Sato, H.; Watanabe, M.; Uematsu, K.; Sato, M.; Toda, K. Near ultraviolet light excitable highly efficient blue-green multicolour warwickite phosphor, ScCaO (BO₃):Ce³⁺, Tb³⁺. *Mater. Adv.* **2023**, *4*, 1546–1554. [[CrossRef](#)]

34. Gracie, P.J.; Geetha, D.; Wahab, H.A.; Battisha, I.K. Structural elucidation by Raman spectroscopy and analysis of luminescence-quenching by the Inokuti-Hirayama model in the Pr³⁺ doped multi-component silicate photonic films. *Opt. Laser Technol.* **2024**, *171*, 110406. [[CrossRef](#)]
35. Wantana, N.; Kaewnuam, E.; Chanthima, N.; Kim, H.J.; Kaewkhao, J. Tuneable luminescence of Pr³⁺-doped sodium aluminium gadolinium phosphate glasses for photonics applications. *Optik* **2022**, *267*, 169668. [[CrossRef](#)]

Disclaimer/Publisher's Note: The statements, opinions and data contained in all publications are solely those of the individual author(s) and contributor(s) and not of MDPI and/or the editor(s). MDPI and/or the editor(s) disclaim responsibility for any injury to people or property resulting from any ideas, methods, instructions or products referred to in the content.